Italian Journal of Zoology
Publication details, including instructions for authors and subscription information:
http://www.tandfonline.com/loi/tizo20

Characterisation of the spherulocyte subpopulations in Eucidaris tribuloides (Cidaroida: Echinoidea)

V. Queiroz[a] & M. R. Custódio[a]
[a] Departamento de Fisiologia Geral, Instituto de Biociências and Núcleo de Apoio à Pesquisa - Centro de Biologia Marinha (NAP-CEBIMar), Universidade de São Paulo, São Paulo, Brazil
Published online: 19 Mar 2015.

To cite this article: V. Queiroz & M. R. Custódio (2015): Characterisation of the spherulocyte subpopulations in Eucidaris tribuloides (Cidaroida: Echinoidea), Italian Journal of Zoology, DOI: 10.1080/11250003.2015.1019580

To link to this article: http://dx.doi.org/10.1080/11250003.2015.1019580

Italian Journal of Zoology, 2015, 1–11
http://dx.doi.org/10.1080/11250003.2015.1019580

Characterisation of the spherulocyte subpopulations in *Eucidaris tribuloides* (Cidaroida: Echinoidea)

V. QUEIROZ* & M. R. CUSTÓDIO

Departamento de Fisiologia Geral, Instituto de Biociências and Núcleo de Apoio à Pesquisa – Centro de Biologia Marinha (NAP–CEBIMar), Universidade de São Paulo, São Paulo, Brazil

(Received 9 September 2014; accepted 2 February 2015)

Abstract
Echinoderms are reported to have up to eight coelomic cell types, but this number can be lower in some classes. In Echinoidea, only three basic types are recognised: phagocytes, vibratile cells and spherulocytes. Most studies on these coelomocytes are based on either live cell suspensions or transmission electron microscopy, while cytochemical studies are scarce. In this work we offer a detailed characterisation of *Eucidaris tribuloides* (Cidaroida: Echinoidea) spherulocytes using an integrative approach (live cells, cytochemistry and transmission electron microscopy). Additionally, evidence on the maturation of these cells is presented. Three distinct spherulocyte types were found in the coelomic fluid: the already-known red and colourless spherulocytes, and a poorly known subpopulation named herein as granular spherulocytes. Three distinct maturation stages could be detected, which are characterised by a remarkable reduction in nuclear diameter while the number and size of cytoplasmic spherules increases.

Keywords: *Coelomocytes, cytochemistry, Echinodermata, maturation, ultrastructure*

Introduction

Echinoderms are group of exclusively marine basal deuterostomes (Edgecombe et al. 2011), characterised by their calcitic skeleton, water vascular system and pentamerous symmetry (Pawson 2007). These animals lack specialised circulatory and respiratory systems, the functions of which are performed by coelomic fluid (Endean 1966). In addition to these roles, the coelom also mediates immune responses, with coelomocytes (free circulating cells in the coelomic cavity) as the main components in this mechanism (Arizza et al. 2007; Smith et al. 2010).

There are records of eight main coelomocyte types in echinoderms, some subdivided into more than one category: phagocytes (or amebocytes), spherulocytes, hemocytes, progenitor (or lymphocytes), crystal, discoidal, polygonal and vibratile cells (for review see Ramírez-Gómez & García-Arrarás 2010). However, some types are restricted to certain groups. For instance, in the Echinoidea (sea urchins), three main cell types can be found: phagocytes, the vibratile cell and the spherulocytes (Smith 1981; Chia & Xing 1995; Smith et al. 2006; Ramírez-Gómez & García-Arrarás 2010). However, the total number of coelomocytes may be higher than we already know. Recent studies on sea urchin phagocytes, using cell markers and confocal microscopy, demonstrated the existence of at least three subpopulations: small phagocytes, discoidal and polygonal cells (Henson et al. 1992, 1999, 2003; Edds 1993; Brockton et al. 2008).

Spherulocytes are characterised by the conspicuous spherical inclusions in the cytoplasm, and are usually divided into two subpopulations. Cells that accumulate naphthoquinone Echinochrome-A are identified as *red* spherulocytes, and the ones containing transparent or hyaline spherules are classified as *colourless* spherulocytes. Nonetheless, some works using transmission electron microscopy (TEM) have found up to five different types of spherule-filled cells (Chien et al. 1970; Vethamany & Fung 1972; Heatfield & Travis 1975).

Despite the fundamental physiological roles attributed to spherulocytes, such as antibacterial activity,

*Correspondence: V. Queiroz, Departamento de Fisiologia Geral, Instituto de Biociências, Universidade de São Paulo, Rua do Matão, nº 321, Cidade Universitária, São Paulo (SP), Brazil. CEP: 05508-090. Tel: +55113091-7522. Fax: +55113091-8095. Email: vinicius_ufba@yahoo.com.br

oxygen transport and cytotoxicity, knowledge on their specific functions is still limited. The chemical nature of compounds in the *colourless* spherules is largely unknown, and even basic data such as their origin and differentiation capabilities are still under debate (Chia & Xing 1995; Silva 2013). Therefore, it would be important to determine spherulocyte types and their structural variability in order to establish cellular differentiation pathways and comprehend their functions.

Most studies on spherulocytes are based either on live cell suspensions or TEM (e.g. Johnson 1969a; Chien et al. 1970; Vethamany & Fung 1972; Bertheussen & Seljelid 1978; Pinsino et al. 2008; McCaughey & Bodnar 2012). However, the lack of correspondence between living cells and electron microscopy preparations could be a major obstacle to the recognition of cell types and the study of their respective functions. Cytochemical procedures are able to combine some inherent qualities of the previous methods, though they are rarely used for this purpose (Liebman 1950; Holland et al. 1965; Johnson 1969b). They allow for the observation of a large number of cells in a single field, as with cell suspensions, and information on the structure and chemical nature of their components can be obtained, which is similar to electron microscopy. Nevertheless, there are no studies integrating all three approaches with Echinoidea spherulocytes. In this context, the aim of this work is to characterise this cell type of the sea urchin *Eucidaris tribuloides* using light microscopy of living and stained cells, and TEM.

Materials and methods

Animals and coelomic fluid collection

Specimens of the cidaroid sea urchin *Eucidaris tribuloides* (Cidaroida: Echinoidea) were collected in the São Sebastião Channel and maintained at room temperature in marine aquaria at the Laboratório de Biologia Celular de Invertebrados Marinhos, Instituto de Biociências–Universidade de São Paulo (IB-USP). The coelomic fluid was collected by inserting a syringe needle preloaded with 1.5 ml of isosmotic anticoagulant solution (20 mM ethylenediamine tetraacetic acid (EDTA), sodium chloride 460 mM, sodium sulfate 7 mM, potassium chloride 10 mM, 4-(2-hydroxyethyl)-1-piperazineethanesulfonic acid (HEPES) 10 mM, pH 8.2; Dunham & Weissman 1986) into the peristomial membrane. An equal volume of coelomic fluid was collected; cells were counted in a Neubauer chamber and density was adjusted to 5×10^5 cells/mL using the same anticoagulant solution.

Light microscopy

Living cell preparations and cytospins were examined. To observe living cells, drops of the suspension were placed in microscopy slides immediately after being obtained and covered with a cover slip. Measurements were taken in 20 cells of each type using a digital imaging system (Opton). Cytospins were prepared using a cytocentrifuge (FANEN 248, 80 µL per spot, 80 × *g*/5 min) and fixed for 45 min in formaldehyde sublimate. These slides were mounted with Entellan (Merck) without further preparations, or stained with toluidine blue, hematoxylin eosin (H&E) and Mallory's trichrome following standard methods (Martoja & Martoja 1967; Behmer et al. 1976). Cell types were determined by the overall shape, nuclear characteristics and cytoplasmic inclusions, following the descriptions in the literature (e.g. Liebman 1950; Holland et al. 1965; Johnson 1969b). Putative maturation stages of each spherulocyte subpopulation were determined according to cytochemical and structural differences of their nuclei and cytoplasmic content. Measurements were performed in the cytospins, 50 cells of each maturation stage, using the same digital imaging system as above.

Transmission electron microscopy (TEM)

Coelomic fluid was collected and fixed in 2.5% glutaraldehyde in anticoagulant solution for 12 h at room temperature. Coelomocytes were then resuspended in anticoagulant solution, embedded in agar 2.5%, centrifuged for 5 min (800 rpm) and post-fixed in osmium tetroxide (1%) with cacodylate buffer for 2 h at 4°C (Taupin 2008). The coelomocytes were then dehydrated in a graded ethanol series (50, 70, 90 e 100%) and embedded in resin (Embed-812, EMS). Ultrathin sections (50–70 nm) were stained with uranyl acetate and lead citrate for 30 and 5 min, respectively, and examined under a Zeiss EM900 electron microscope.

Statistical analyses

Data on nucleus, cytoplasm and spherule diameter of live and unstained cells are presented as mean ± standard deviation for larger structures or minimum–maximum diameters for smaller ones. Nuclear diameters of stained preparations are presented as mean ± standard deviation. One-way analysis of variance (ANOVA; GraphPad InStat Statistical Software v. 3.0) was used to test differences among nucleus diameters of different maturation stages (early, intermediate

and final) in each cell type. Differences are considered significant at a probability level of 0.05.

Results

Three distinct spherulocyte types could be identified in the coelomic fluid: red spherulocytes, colourless spherulocytes and a poorly known subpopulation named herein as granular spherulocytes. For each of these cell types, a continuous maturation process could be observed, which was divided into three main stages: *early* (largest nucleus diameter and cytoplasm reticulated and/or without spherules); *intermediate* (nucleus diameter decreases, whereas the cytoplasm is filled and becomes increasingly spherulous); and *final* (smaller nucleus diameter, commonly peripheral, and cytoplasm filled with many spherules). The nucleus diameter among the three stages of all spherulocyte types differs statistically ($P < 0.05$; Figure 1).

Red spherulocytes

Living cells (Figure 2a) *and unstained preparations* (Figure 2d): The live cells display a spherical to oval shape (diameter = 11.58 ± 2.77 μm). The nucleus is round (3.1–3.8 μm), and often eccentric when visible. The cytoplasm is filled with spherules ranging between 1.21 and 1.42 μm, and containing the red pigment Echinochrome-A (Figure 2a). When these cells are handled without anticoagulant solution, they show an elongated shape with amoeboid movements. Unstained cells have a reddish peripheral nucleus and a flat, brown, disorganised cytoplasm (Figure 2d).

Stained preparations: Early stage (Figure 3a, g and m): Nucleus (diameter = 5 ± 0.43 μm) usually condensed, central and with high affinity for toluidine blue. It does not stain with other dyes, but shows a reddish colouration probably due to the presence of Echinochrome-A. Cytoplasm rather spread with a characteristic reticulated appearance. Intermediate stages (Figure 3b–e, h–k and n–q): Nucleus (diameter = 3.9 ± 0.43 μm) with strong affinity to toluidine blue, slightly condensed and eccentric (peripheral in some cases) presenting a small nucleolus (Figure 3e). Cytoplasm is dispersed and the initial reticulated appearance decreases during maturation, while there is an increase in the spherules that stain only in toluidine blue. Final stage: Small peripheral nucleus (2.8 ± 0.39 μm) with less affinity to toluidine blue than the surrounding cytoplasm, and slightly eosinophilic/acidophilic with remaining stains. Cytoplasm with many spherules showing high affinity to toluidine blue, but only slightly eosinophilic/acidophilic with remaining stains (Figure 3f, l and r).

Transmission electron microscopy (Figure 4a–d): Cells are oval, and the large irregular nucleus is always peripheral (Figure 4a–c). Chromatin is mostly condensed (heterochromatin; Figure 4c), distributed in clumps, sometimes presenting a nucleolus. Cytoplasm showed apparently empty vacuoles in some cells, while in others they were filled with a large number of spherules of different sizes with electron-dense contents (Figure 4a–c). A large number of mitochondria (Figure 4c, d), a well-developed Golgi complex and blunt pseudopodia (Figure 4a, b) could be observed. The possible maturation sequence, with early, intermediate and final stages

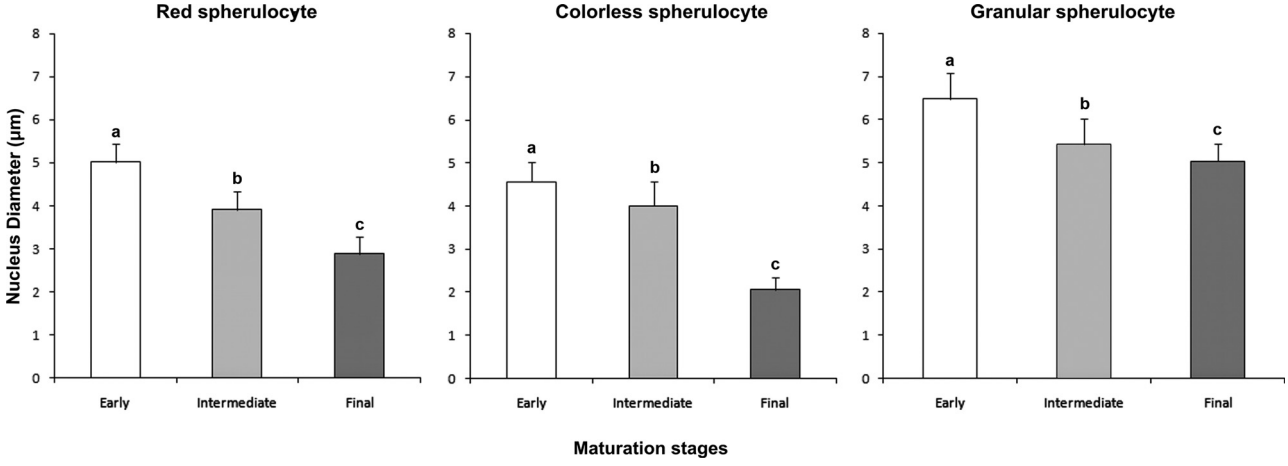

Figure 1. Nucleus diameter of the spherulocytes found in *Eucidaris tribuloides*. In each cell type, distinct letters show significant differences ($p < 0.05$).

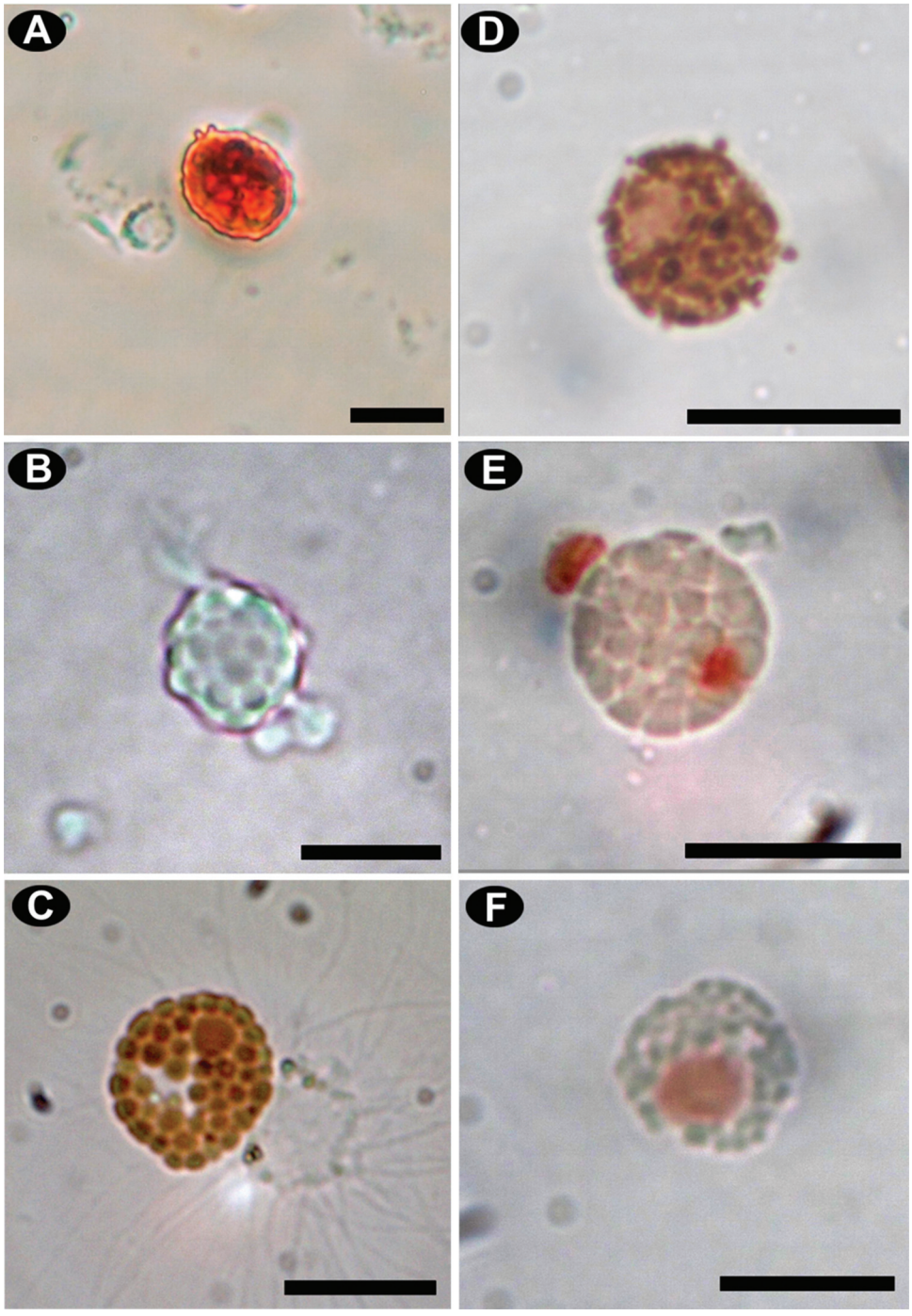

Figure 2. Live (A–C) and fixed unstained (D–F) spherulocytes. (A) and (D): red spherulocyte; (B) and (E): colourless spherulocyte; (C) and (F): granular spherulocyte. Scale bar: 10 μm.

corresponding to what was observed in stained cells, could also be detected (Figure 4a–c).

Colourless spherulocytes

Living cells (Figure 2b) *and unstained preparations* (Figure 2e): Spherical to oval shape (diameter 12.36 ± 1.1 μm). The nucleus is round (3.2–3.8 μm) and often eccentric. The cytoplasm is slightly flattened and filled with colourless spherules of unknown content, whose diameter ranged from 2.07 to 2.40 μm (Figure 2b). Morphology is similar to that of red spherulocytes, showing an elongated shape and amoeboid movements when handled

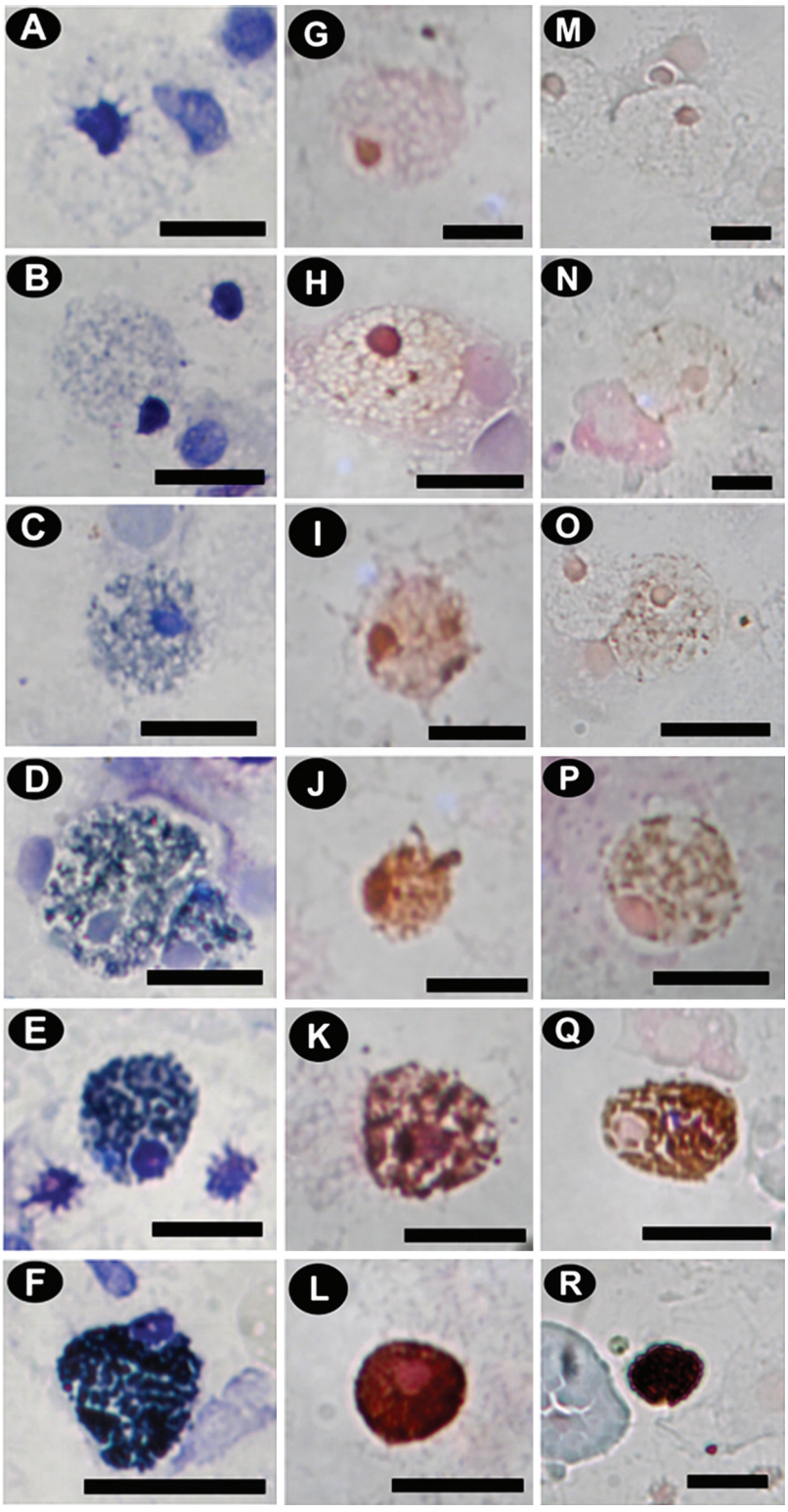

Figure 3. Stained red spherulocytes in different stages of the putative maturation process. (A), (G) and (M): early stage; (B–E), (H–K) and (N–Q): intermediate stage; (F), (L) and (R): final stage. (A–F): toluidine blue; (G–L): hematoxylin and eosin; (M–R): Mallory trichrome. Scale bar: 10 μm.

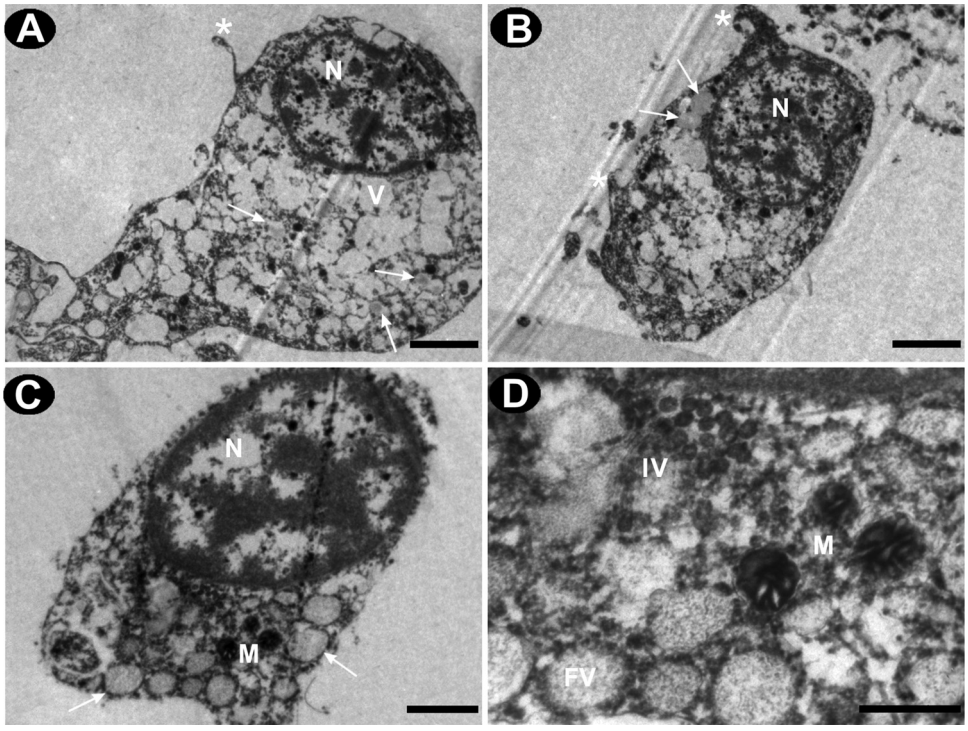

Figure 4. Transmission electron microscopy of the red spherulocyte in different maturation stages. (A): early; (B): intermediate; (C): final; (D): detail of a cell in the final stage (M = mitochondria; N = nucleus; V = empty vacuole; IV = initial vacuole; FV = final vacuole; Arrow = full vacuole; Asterisk = blunt pseudopodia). Scale bars: (A) and (B), 2 μm. (C), 1 μm. (D), 0.5 μm.

without anticoagulant solution. Unstained cells have a reddish peripheral nucleus and a greenish, organised cytoplasm (Figure 2e).

Stained preparations: Early stage (Figure 5a, e and i): Nucleus eccentric, poorly condensed, measuring 4.5 ± 0.46 μm and with high affinity to toluidine blue and H&E. Cytoplasm dispersed, without a clear boundary and very reticulated; reticules are larger than in early red spherulocytes and without affinity to any dye. Intermediate stage (Figure 5b–c, f–g and j–k): Nucleus smaller than previous stage (4 ± 0.54 μm), peripheral and poorly condensed, with a nucleolus sometimes visible. It also does not present affinity to Mallory's trichrome. The cytoplasm is homogeneously dispersed but loses this characteristic through maturation and becomes visibly more compact and spherulous. It shows an affinity to H&E and to the methyl blue dye present in the Mallory's trichrome. Final stage (Figure 5d, h and l): Small nucleus commonly centralised and condensed, measuring 2.6 ± 0.27 μm. Cytoplasm organised, showing well-developed spherules with roughly the same affinity as the previous stage, but with a darker central core (Figure 5l).

Transmission electron microscopy (Figure 6a–d): Cell rounded in shape with a small peripheral nucleus (Figure 6a). The cytoplasm shows a large number of vacuoles, filled with a centralised electron-dense material. Mitochondria, rough endoplasmic reticulum and a large Golgi apparatus were also present (Figure 6b–d). It was also possible to observe some vesicle development next to the Golgi complex, in which a central core is formed and becomes more electron-dense (Figure 6d).

Granular spherulocytes

Living cells (Figure 2c) *and unstained preparations* (Figure 2f): Only a few cells were observed, all displaying a round shape and approximately 12.2 μm diameter. Nucleus was 3.4–4.0 μm, round and often peripheral. Cytoplasm is filled with large spherules containing a brownish content of unknown composition, measuring 1.3–1.9 μm in diameter (Figure 2c). No amoeboid movements were observed in living cells. Unstained cells show a large reddish peripheral nucleus and an organised cytoplasm filled with well-delimited green spherules (Figure 2f).

Stained preparations: Early stage (Figure 7a, d and g): The nucleus is large, rounded, centralised and poorly condensed, measuring 6.4 ± 0.58 μm and with a slight affinity to toluidine blue and H&E. Cytoplasm is compact, with a clear boundary and presenting a homogeneous appearance. It shows no

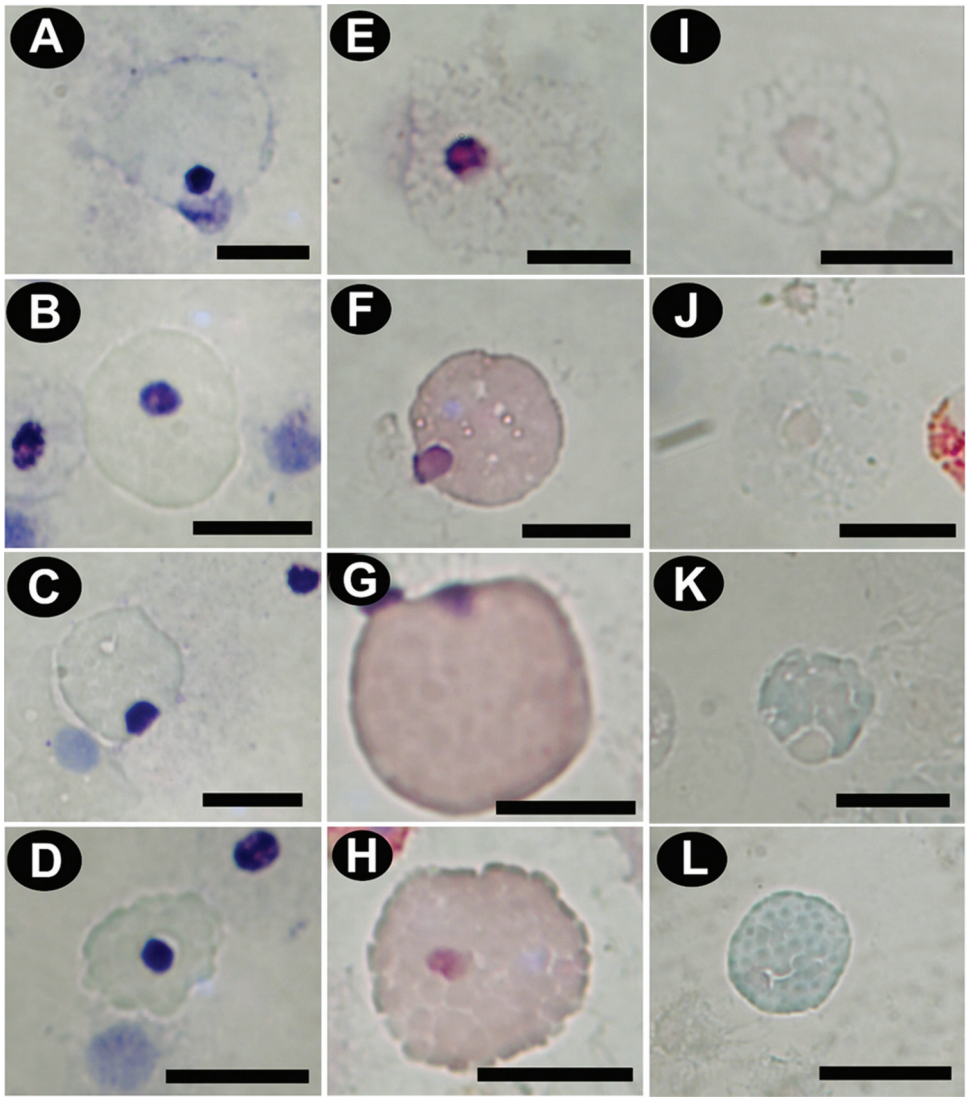

Figure 5. Stained colourless spherulocyte in different maturation stages. (A), (E), and (I): early stage; (B–C), (F–G) and (J–K): intermediate stage; (D), (H) and (L): final stage. (A–D): toluidine blue; (E–H): hematoxylin and eosin; (I–L): Mallory's trichrome. Scale bar: 10 μm.

affinity to toluidine blue, with a greyish/yellowish colour, and it stains slightly with H&E and acid fuchsine present in the Mallory's trichrome. Intermediate stage (Figure 7b, e and h): The nucleus diameter is smaller than in the previous stage (5.4 ± 0.6 μm), and it is commonly placed in the periphery, with intermediate affinity to toluidine blue and slight affinity to the other stains. The cytoplasm shows the beginning of the spherule formation and it has an affinity to acid fuchsine and H&E, but not to toluidine blue. Final stage (Figure 7c, f and i): Nucleus always peripheral and more condensed, 5 ± 0.38 μm in diameter. Cytoplasm organised, showing well-developed and individualised spherules containing an unidentified material showing high affinity to acid fuchsine.

Transmission electron microscopy (Figure 8a–e): Cells are oval or round, and the large, regular nucleus is generally peripheral, at least in intermediate and final stages (Figure 8c–e). The chromatin is condensed, distributed in clumps, and a nucleolus was common, sometimes with an electron-dense structure (Figure 8d). The cytoplasm is filled with spherules of high electron-dense content whose diameter increases probably due to vesicular fusion along maturation process (Figure 8a–e). A large number of mitochondria, ribosomes (polyribosome and free ribosomes) and rough endoplasmic reticulum were present. It was also possible to observe a maturation sequence similar to those in stained preparations: early (Figure 8a and b), intermediate (Figure 8c and d) and final stages (Figure 8e).

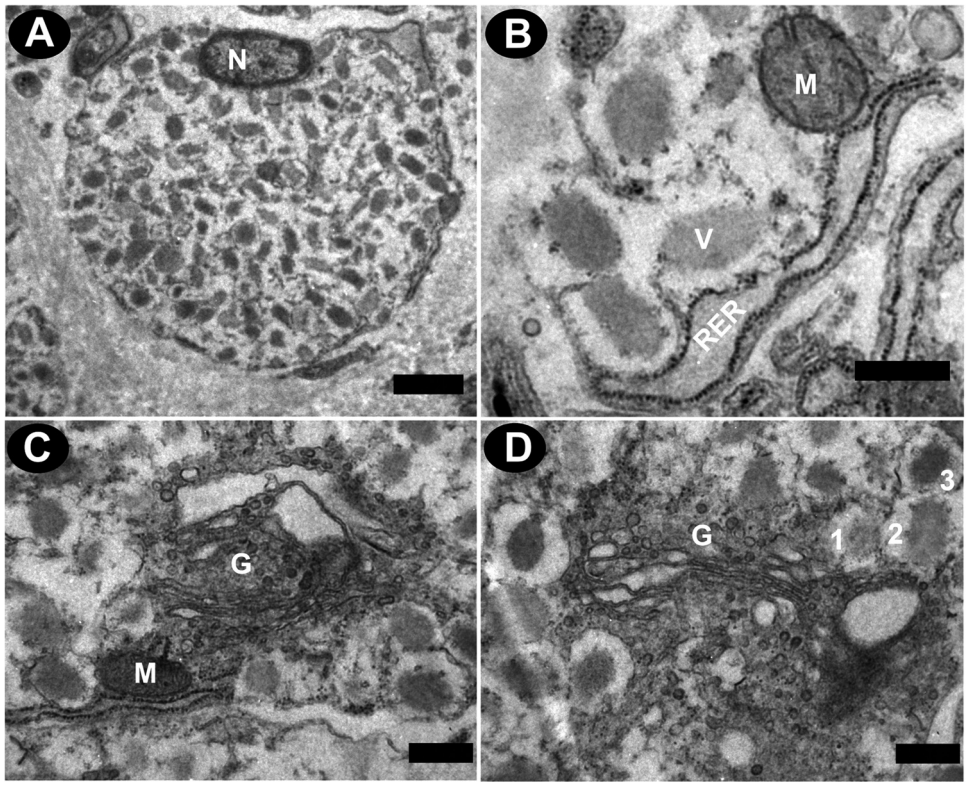

Figure 6. Transmission electron microscopy of a colourless spherulocyte. (A): cell overview; (B): detail of the spherules; (C): Golgi complex; (D): Golgi complex with different stages of spherule formation (G = Golgi complex; M = mitochondria; N = nucleus; RER = rough endoplasmic reticulum; V = empty vacuole; 1–3 = spherule maturation. Scale bars: (A), 2 μm. (B–D), 0.5 μm.

Discussion

Since the classical work of Metchnikoff (1893) on phagocytosis, many studies were made in an attempt to identify and describe echinoderm coelomocytes (Kindred 1921, 1924; Boolootian & Geise 1958; Endean 1966). However, only live cells in suspension and/or TEM have been largely used, while cytochemical studies have been very scarce and observations of fixed unstained cells were never performed.

The cytochemical approach using cytospins allowed for the acquisition of new data on coelomocyte development (maturation stages, cf. Figures 2, 5 and 7). It was difficult to establish comparisons with previous works due to the wide variation in techniques. As stated before, "fixatives have a profound effect on both staining and cytochemical reactions of the spherule cells" (Johnson 1969b: 225). Nevertheless, the nucleus and cytoplasm morphology are more stable and therefore useful to identify this cell type.

The general characteristics of the red and colourless spherulocytes observed in *E. tribuloides* are similar to those described for other Echinoidea (Liebman 1950; Johnson 1969a; Bertheussen & Seljelid 1978; Matranga et al. 2006; McCaughey & Bodnar 2012). The red spherulocyte presented the same "flat" aspect described for *Arbacia punctata* (Liebman 1950), and similar colouration was found in spherulocytes named "Type I" from two species of the genus *Strongylocentrotus* (Johnson 1969b). The same characteristics are described for *S. purpuratus*, although it presents a sub-central euchromatic nucleus and the content of the spherules was not visible, with a few of them presenting either a crystalline or a coarse material (Heatfield & Travis 1975).

The colourless spherulocyte stained with Mallory's trichrome was also similar to the one found in *A. punctata* (Liebman 1950) and to the granulocyte of *S. purpuratus* (Heatfield & Travis 1975). The morphology compares well with the "Type II" spherulocytes from *Strongylocentrotus* species (Johnson 1969b). On the other hand, the ultrastructure of the colourless spherule of *E. tribuloides* was different from those observed in *S. dröebachiensis*, *S. purpuratus* and *Heliocidaris erythrogramma* (Vethamany & Fung 1972; Heatfield & Travis 1975; Dheilly et al. 2011, respectively). In *S. dröebachiensis*, the cytoplasmic spherules were apparently empty, and only mitochondria were identified (Vethamany & Fung 1972). Meanwhile, in *S. purpuratus* and *H. erythrogramma*, most spherules were

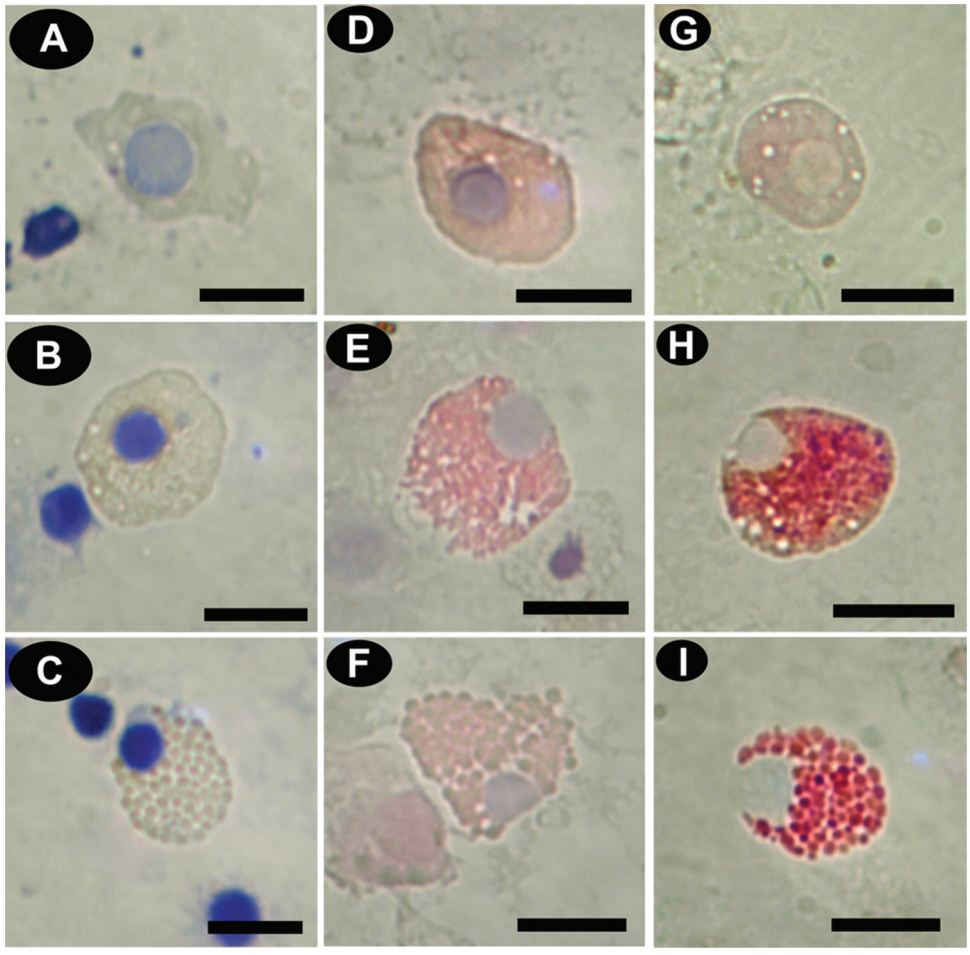

Figure 7. Stained granular spherulocyte in different maturation stages. (A), (D) and (G): early stage; (B), (E) and (H): intermediate stage; (C), (F) and (I): final stage. (A–C): toluidine blue; (D–F): hematoxylin and eosin; (G–I): Mallory's trichrome. Scale bar: 10 μm.

completely filled by a highly electron-dense material (Heatfield & Travis 1975; Dheilly et al. 2011). Furthermore, in *S. purpuratus*, four spherule types could be observed (named S_1 to S_4), and some of them showed a membranous material. Unlike these species, the colourless spherulocyte of *E. tribuloides* presented only one type of spherule with a slightly central electron dense material (cf. Figure 6).

The granular spherulocyte is very different from the other two types. Its spherules are well defined and its nucleus was always visible (cf. Figure 2c). This cell is similar in morphology to the "green spherulocyte" observed in *A. punctata* (Liebman 1950). However, the spherule content is distinct and cells with strong (*lemon*) green colour, as described for *A. punctata*, were not observed. The staining reactions to the granular spherulocyte of *E. tribuloides* were very singular. In toluidine blue preparations the spherules do not stain, showing only a greyish/yellowish colour, but they do react with other dyes. In the few studies using cytochemical procedures (Liebman 1950; Holland et al. 1965; Johnson 1969b), there is no reference to a cell with these features. A cell type with the ultrastructure similar to the final stage of the granular spherulocyte of *E. tribuloides* was described for *S. dröebachiensis*, and named *granulocyte* (Vethamany & Fung 1972). There is also a similar record for *S. purpuratus* (Heatfield & Travis 1975). Nevertheless, it is completely different from that found in *S. dröebachiensis* (Vethamany & Fung 1972). However, differently from *S. dröebachiensis*, this cell is not rare in *E. tribuloides*, and was found frequently in stained and electron microscopy preparations. It is possible that the cells described for *S. drobachiensis* represent only initial stages, with small cytoplasmic inclusions (*granules*. cf. Figure 8a), and further stages were not described.

In addition to the analysis of cytochemical and ultrastructural characteristics, nucleus measures can also corroborate the maturation process observed here. Changes in nucleus size can be directly related

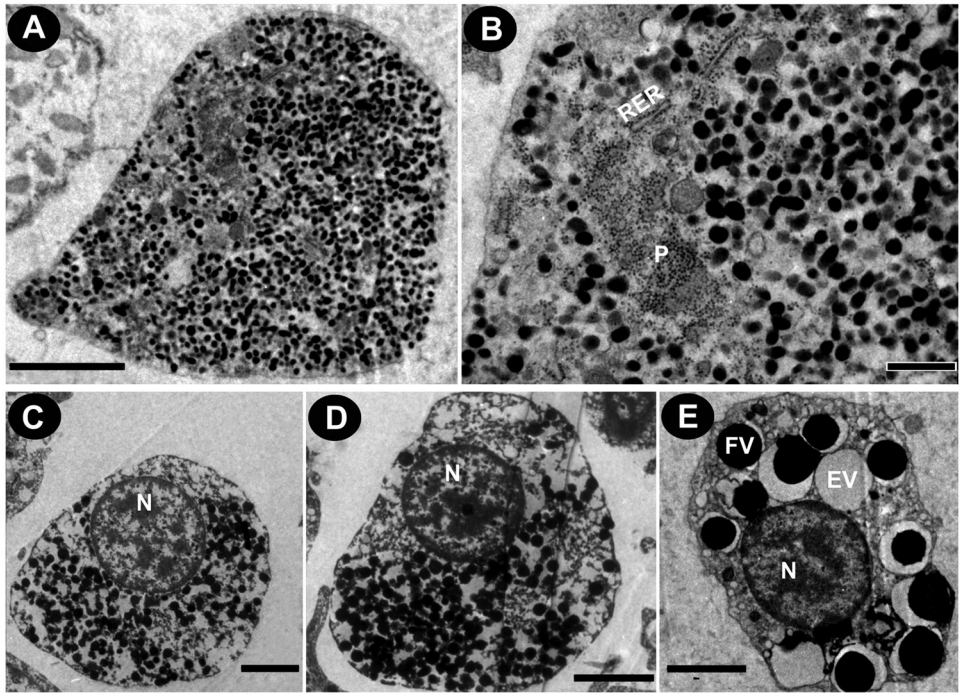

Figure 8. Transmission electron microscopy of the granular spherule cell in different maturation stages. (A) and (B): early; (C) and (D): intermediate; (E): final (EV = empty vacuole; FV = full vacuole; N = nucleus; P = polyribosomes; RER = rough endoplasmic reticulum). Scale bars: (A), (C–E), 2 μm. (B), 0.5 μm.

to RNA transcription levels (Sato et al. 1994; Schmidt & Schibler 1995; Webster et al. 2009) and this fits into the dynamics of *E. tribuloides* spherulocytes. The cells in the first stage contain empty spherules and a large nucleus, evidence of intense RNA production, while the mature stage shows full vacuoles and a small, condensed nucleus, indicating a decrease in transcription. A similar pattern was also described for holothurian hemocytes, whose nucleus size was larger in very immature cells, intermediate in immature and smaller in mature ones (Fontaine & Hall 1981). Additionally, the granular spherulocyte maintains a larger nuclear size in the final stage when compared with the other two types (cf. Figure 1). This can indicate that this cell does not reduce its transcription process and therefore has a different role from the other spherulocytes (production/release vs. production/storage?).

The lack of studies combining different techniques and the coexistence of cell types with two widely different morphologies between the early and final stages of maturation could explain the variation in the number of spherulocyte subpopulations detected in Echinodermata (Chien et al. 1970; Vethamany & Fung 1972; Heatfield & Travis 1975). Before trying to understand the roles of these cells in echinoderm physiology, it is important to know how many subpopulations there are in fact. As shown in this study, an integrative approach may be a useful tool to solve this problem.

Acknowledgements

The authors thank Dr. Alberto de Freitas Ribeiro and Waldir Caldeira (LME, Laboratório de Microscopia Eletrônica – IB-USP) for providing equipment and support with transmission electron microscopy, and the staff of CEBIMar (USP) for the provision of laboratory facilities and technical support during field trips. We also thank to Daniel C. Cavalary for English revision.

References

Arizza V, Giaramita F, Parrinello D, Cammarata M, Parrinello N. 2007. Cell cooperation in coelomocyte cytotoxic activity of *Paracentrotus lividus* coelomocytes. Comparative Biochemistry and Physiology Part A: Molecular & Integrative Physiology 147:389–394. doi:10.1016/j.cbpa.2007.01.022.

Behmer OA, Tolosa EMC, Freitas-Neto AG. 1976. Manual de técnicas de histologia normal e patológica. São Paulo: EDART/EDUSP.

Bertheussen K, Seljelid R. 1978. Echinoid phagocytes *in vitro*. Experimental Cell Research 111:401–412. doi:10.1016/0014-4827(78)90185-4.

Boolootian RA, Geise CA. 1958. Coelomic corpuscles of echinoderms. Biological Bulletin 115:53–56. doi:10.2307/1539092.

Brockton V, Henson JH, Raftos DA, Majeske AJ, Kim Y, Smith LC. 2008. Localization and diversity of 185/333 proteins from

the purple sea urchin – unexpected protein-size range and protein expression in a new coelomocyte type. Journal of Cell Science 121:339–348. doi:10.1242/jcs.012096.

Chia F, Xing J. 1995. Echinoderm coelomocytes. Zoological Studies 35:231–254.

Chien PK, Johnson PT, Holland ND, Chapman FA. 1970. The coelomic elements of sea urchins (*Strongylocentrotus*) IV. Ultrastructure of the coelomocytes. Protoplasma 71:419–442. doi:10.1007/BF01279686.

Dheilly NM, Birch D, Nair SV, Raftos DA. 2011. Ultrastructural localization of highly variable 185/333 immune response proteins in the coelomocytes of the sea urchin, *Heliocidaris erythrogramma*. Immunology and Cell Biology 89:861–869. doi:10.1038/icb.2011.3.

Dunham P, Weissman G. 1986. Aggregation of marine sponge cells induced by Ca pulses, Ca ionophores, and phorbol esters proceeds in the absence of external Ca. Biochemical and Biophysical Research Communications 134:1319–1326. doi:10.1016/0006-291X(86)90394-3.

Edds KT. 1993. Cell biology of echinoid coelomocytes. Journal of Invertebrate Pathology 61:173–178. doi:10.1006/jipa.1993.1031.

Edgecombe GD, Giribet G, Dunn CW, Hejnol A, Kristensen RM, Neves RC, Rouse GW, Worsaae K, Sørensen MV. 2011. Higher-level metazoan relationships: Recent progress and remaining questions. Organisms Diversity & Evolution 11:151–172. doi:10.1007/s13127-011-0044-4.

Endean R. 1966. The coelomocytes and coelomic fluids. In: RA Boolootian, editor. Physiology of Echinodermata. New York, NY: Interscience. 301–328.

Fontaine AR, Hall BD. 1981. The haemocyte of the holothurian *Eupentacta quinquesemita*: Ultrastructure and maturation. Canadian Journal of Zoology 59:1884–1891. doi:10.1139/z81-256.

Heatfield BM, Travis DF. 1975. Ultrastructural studies of regenerating spines of the sea urchin *Strongylocentrotus purpuratus*. II. Cell types with spherules. Journal of Morphology 145:51–71. doi:10.1002/jmor.1051450104.

Henson JH, Kolnik SE, Fried CA, Nazarian R, McGreevy J, Schulberg KL, Detweiler M, Trabosh VA. 2003. Actin-based centripetal flow: Phosphatase inhibition by calyculin-A alters flow pattern, actin organization and actomyosin distribution. Cell Motility and the Cytoskeleton 56:252–266. doi:10.1002/cm.10149.

Henson JH, Nesbitt D, Wright BD, Scholey JM. 1992. Immunolocalization of kinesin in sea urchin coelomocytes. Association of kinesin with intracellular organelles. Journal of Cell Science 103(Pt 2):309–320.

Henson JH, Svitkina TM, Burns AR, Hughes HE, MacPartland KJ, Nazarian R, Borisy GG. 1999. Two components of actin-based retrograde flow in sea urchin coelomocytes. Molecular Biology of the Cell 10:4075–4090. doi:10.1091/mbc.10.12.4075.

Holland ND, Phillips JH, Giese AC. 1965. An autoradiographic investigation of coelomocyte production in the purple sea urchin (*Strongylocentrous purpuratus*). Biological Bulletin 128:259–270. doi:10.2307/1539554.

Johnson PT. 1969a. The coelomic elements of sea urchins (*Strongylocentrotus*). I. The normal coelomocytes; their morphology and dynamics in hanging drops. Journal of Invertebrate Pathology 13:25–41. doi:10.1016/0022-2011(69)90236-5.

Johnson PT. 1969b. The coelomic elements of sea urchins (*Strongylocentrotus*) II. Cytochemistry of the Coelomocytes. Histochemie 17:213–231. doi:10.1007/BF00309866.

Kindred JE. 1921. Phagocytosis and clotting in the perivisceral fluid of *Arbacia*. Biological Bulletin 41:144–152. doi:10.2307/1536745.

Kindred JE. 1924. The cellular elements in the perivisceral fluid of echinoderms. Biological Bulletin 46:228–251. doi:10.2307/1536725.

Liebman E. 1950. The leucocytes of *Arbacia punctulata*. Biological Bulletin 98:46–59. doi:10.2307/1538598.

Martoja R, Martoja M. 1967. Initiation aux Techniques de l'Histologie Animale. Paris: Masson et Cie. 354 pp.

Matranga V, Pinsino A, Celi M, Di-Bella G, Natoli A. 2006. Impacts of UV-B radiation on short-term cultures of sea urchin coelomocytes. Marine Biology 149:25–34. doi:10.1007/s00227-005-0212-1.

McCaughey C, Bodnar A. 2012. Investigating the sea urchin immune system: Implications for disease resistance and aging. Journal of Young Investigator 23:25–33.

Metchnikoff E. 1893. Lectures on the comparative pathology of inflammation: Delivered at the pasteur institute in 1891. London: Kegan Paul, Trench, Trubner & Co. Ltd.

Pawson DL. 2007. Phylum Echinodermata. Zootaxa 1668:749–764.

Pinsino A, Della-Torre C, Sammarini V, Bonaventura R, Amato E, Matranga V. 2008. Sea urchin coelomocytes as a novel cellular biosensor of environmental stress: A field study in the Tremiti Island Marine Protected Area, Southern Adriatic Sea, Italy. Cell Biology and Toxicology 24:541–552. doi:10.1007/s10565-008-9055-0.

Ramírez-Gómez F, García-Arrarás JE. 2010. Echinoderm immunity. Invertebrate Survival Journal 7:211–220.

Sato S, Burgess SB, McIlwain DL. 1994. Transcription and motoneuron size. Journal of Neurochemistry 63:1609–1615. doi:10.1046/j.1471-4159.1994.63051609.x.

Schmidt EE, Schibler U. 1995. Cell size regulation, a mechanism that controls cellular RNA accumulation: Consequences on regulation of the ubiquitous transcription factors Oct1 and NF-Y and the liver-enriched transcription factor DBP. Journal of Cell Biology 128:467–483. doi:10.1083/jcb.128.4.467.

Silva JRMC. 2013. Immunology in Sea Urchins. In: JM Lawrence, editor. Sea Urchins: Biology and ecology. 3rd ed. San Diego, CA: Academic Press. pp. 187–194.

Smith CL, Ghosh J, Buckley KM, Clow LA, Dheilly NM, Huag T, Henson JH, Cheng Man Lun CL, Majeske AJ, Matranga V, Nair SV, Rast JP, Raftos DA, Roth M, Sacchi S, Schrankel CS, Stensvag K. 2010. Echinoderm immunity. In: Söderhäll K, editor. Invertebrate immunity. New York, NY: Landes Bioscience and Springer Science Business Media. pp. 260–301.

Smith LC, Rast JP, Brockton V, Terwilliger DP, Nair SV, Buckley KM, Majeske AJ. 2006. The sea urchin immune system. Invertebrate Survival Journal 3:25–39.

Smith VJ. 1981. The echinoderms. In: Ratcliffe NA, Rowley AF, editors. Invertebrate blood cells. New York, NY: Academic Press. pp. 513–562.

Taupin P. 2008. Electron microscopy of cell suspension. Annals of Microscopy 8:19–21.

Vethamany VG, Fung M. 1972. The fine structure of coelomocytes of the sea urchin, *Strongylocentrotus dröbachiensis* (Müllier O.F.). Canadian Journal of Zoology 50:77–81. doi:10.1139/z72-014.

Webster M, Witkin KL, Cohen-Fix O. 2009. Sizing up the nucleus: Nuclear shape, size and nuclear-envelope assembly. Journal of Cell Science 122:1477–1486. doi:10.1242/jcs.037333.